EAST EUROPEAN JOURNAL OF PHYSICS. **2.** 520-527 (2026)
DOI:10.26565/2312-4334-2026-2-59 ISSN 2312-4334

CHARACTERISTICS OF RADIATED FIELDS FORMED BY PATCH ANTENNA WITH COMPLICATED APERTURE

Sergey A. Pogarsky*, Dmitry V. Mayboroda, Mikhail V. Nesterenko, Serhii M. Mykhaliuk, Oleksander A. Biloshenko
V.N. Karazin Kharkiv National University, 4, Svobody Sq., Kharkiv, Ukraine, 61022
**Corresponding Author e-mail: spogarsky@gmail.com*
Received March 9, 2026; revised May 2, 2026; accepted May 20, 2026

The paper considers issues related to simulating the electrodynamic characteristics of a patch antenna based on a microstrip disc resonator with a complex topology of the radiating aperture in the form of three slot log-periodic discontinuities, oriented at an angle of 120° with the scaling factor $\tau = 0.8$ and the spacing factor $\sigma = 0.15$. Three concentric ring slot discontinuities are located in a grounded base at a certain distance from the dielectric substrate, the centers of which coincide with the center of the microstrip disc. The antenna was fed by a section of a coplanar line with a stepped profile of the central conductor. The calculations used two methods: the magnetic wall model (semi-open resonator model) and the finite element method. After optimization procedures were carried out for the selected parameters, it was established that compromise parameter sets were necessary to obtain the required characteristics.
Keywords: *Ring resonator; Slot discontinuity; Coplanar line; Matching; Frequency characteristics; Energy characteristics*
PACS: 84.40.Ba; 41.20.Jb

Patch monopole antennas, which appeared in the mid-20th century, became a fundamental design for creating radiating systems for various purposes, thanks to their simplicity, low cost, relatively straightforward matching, and fairly easy parameter optimization. Since their appearance, the design of such antennas has been constantly evolving. This process affects not only changes in the topology of radiating elements – from the simplest canonical forms (rectangular, circular, ring-shaped, and their modifications) [1-3] to fairly complex ones in terms of topology (including fractal ones) [4-12], but also the process of searching for and using new substrate materials with unique characteristics [13-15]. A separate niche is occupied by so-called conformal antennas [16-18], whose geometry is matched to the curved surfaces on which they are placed.

The directions of antenna modifications were almost always determined by the need to solve specific problems. This was either the formation of specific directional patterns [19-21], or the creation of designs that provided the radiation (reception) of signals with circular polarization [22-24], or ensuring high gain values [25, 26], or ensuring the reconfigurability of the antenna design through the use of semiconductor elements [27, 28], and others. However, in solving all these problems, the important issue remained ensuring an acceptable level of antenna matching to external circuits.

Recently, there has been a real need to develop so-called 'wearable' small-sized antennas for both individual identification and common communication tasks [29, 30]. Given the specifics of this type of task, at least two non-standard requirements for the characteristics of such antennas can be formulated. The first requirement is that, depending on the antenna's location, the surface's radius of curvature at that location must be taken into account. This factor will be particularly relevant when the antenna's geometric dimensions increase relative to the wavelength. In cases where the geometric dimensions of the antenna are comparable to (or smaller than) the wavelength, flat antennas can be considered. The second requirement concerns the need to form a specific directional pattern. The specificity is that reception (radiation) in a direction perpendicular to the antenna plane is not predominant. The reason is that the transmitter (receiver) will almost always be at some angle of elevation above the horizon (above the antenna plane). Of course, with all this, it is necessary to ensure satisfactory matching with external circuits. It is desirable to ensure circular (elliptical) polarization within a certain angle range and a sufficiently high antenna gain.

It is clear that such a set of requirements cannot be implemented using trivial (classical) designs. It can be assumed that the potential design should have both a sufficiently non-trivial topology of the radiating aperture and additional design elements that enable the formation of the required directional pattern.

In this paper, the results of a simulation of the characteristics of a planar monopole antenna with a complex radiating aperture topology consisting of three slot log-periodic radiators oriented at an angle of 120° to each other, and a grounding screen with a set of slot discontinuities in the form of concentric circles, are presented. The antenna was fed using a section of a coplanar line.

STRUCTURE UNDER CONSIDERATION

We will consider a monopole planar antenna, the design of which is based on a disc microstrip resonator with three slot apertures in the form of log-periodic elements oriented at an angle of 120° with a scale factor $\tau = 0.8$ and a

Cite as: S.A. Pogarsky, D.V. Mayboroda, M.V. Nesterenko, S.M. Mykhaliuk, O.A. Biloshenko, East Eur. J. Phys. 2, 520 (2026), https://doi.org/10.26565/2312-4334-2026-2-59

spacing factor $\sigma = 0.15$. The element standard for all microstrip structures – a grounded base – is located at a certain distance from the dielectric substrate. It is assumed that the geometric dimensions of the grounded base significantly exceed the geometric dimensions of the substrate, and they are significantly larger than the wavelength. This choice of dimensions eliminates specific effects (diffraction effects at the edges of metal elements and the so-called 'flow' of currents to the opposite side of the grounded plane). The grounded base has three concentric slot irregularities, the geometric centers of which coincide with the geometric center of the disc resonator. The width of the slot elements is 1 mm, and the radii are selected so that the slot discontinuities intersect the projections of the log-periodic apertures in three characteristic areas. The antenna is fed using a section of a coplanar line, the inner conductor of which has a stepped profile. The antenna design is shown in Fig. 1. Fig. 1a – the image of antenna, Fig. 1b – the topology of aperture on the top part of the substrate, Fig. 1c – the grounded base with concentric slot discontinuities.

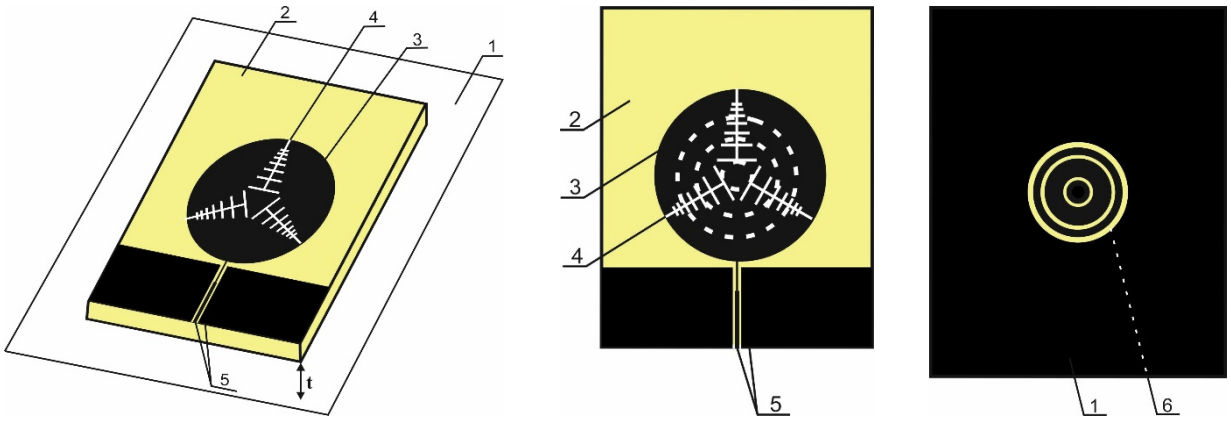

a) b) c)

Figure 1. The design of the antenna

The following symbols are used in the figure: 1 – grounded base, 2 – dielectric substrate, 3 – disc resonator, 4 – log-periodic discontinuities, 5 – coplanar elements, 6 – additional slot discontinuities in the metalized screen

The geometric dimensions of the disc resonator and the material constants of the dielectrics were selected based on the assumption that the antenna would operate in the microwave range. The use of slot discontinuities in the screen provides additional opportunities for solving problems such as matching the antenna to external circuits and adjusting the antenna's energy characteristics (directivity pattern, gain coefficient, and polarization characteristics). The gap between the dielectric substrate and the grounded base is easily achieved by using an additional dielectric layer. In cases where the required characteristics are achieved at $\varepsilon_r = 1$, it is possible to use special dielectrics, such as expanded polystyrene foam or polyurethane foam with parameters $\varepsilon_r = 1.02...1.06$ and $tg\,\delta = (1...5)10^{-4}$ (the parameters remain virtually unchanged in the frequency range from 100 MHz to 10 GHz). It is assumed that the conductivity of all metal elements is infinite (ideal metal).

NUMERICAL MODELLING RESULTS

Complete information about the electrodynamic characteristics of any electrodynamic structure can only be obtained by solving the corresponding boundary value problem formulated for a model that takes into account the maximum set of factors and features of the object itself. The antenna under consideration is a rather complex 3D structure, which makes it extremely difficult to build a model that takes all factors into account. In this situation, it can be argued that a rigorous solution to such an electrodynamic problem, which is currently unavailable, is unlikely to be found in the near future. A realistic solution in this situation is numerical simulating of the antenna's characteristics based on a model that takes into account the most significant parameters and the relationships between them. An important step in constructing such a model is to identify the most characteristic variable parameters, which are used to optimize the characteristics. However, it should be noted that the optimal set of parameters obtained for a particular antenna characteristic does not guarantee the optimality of other antenna characteristics.

The complexity of constructing a generalized model lies in the fact that the structure is a combination of resonators. In the plane of the microstrip patch, the first resonances are those of the aperture of the microstrip disc itself, and the second are those of the slot discontinuities. Resonance may also occur in the dielectric substrate and in the gap between the substrate and the grounded base (especially with increasing frequency). In the grounded base itself, where the ring slot discontinuities are located, resonances may occur at certain frequencies. Resonances in the coplanar line segment can be disregarded, since it has relatively small linear dimensions, which shifts the resonance frequencies beyond the range under consideration. The overall characteristics of the antenna will be formed taking into account all these factors, which is why it is mandatory to optimize the parameters according to the selected variable parameters.

It is obvious that the optimal model cannot be based on the use of only one approach or method (even numerical), since such implementation would lead to high demands on computer resources and calculation time. The most rational

approach seems to be the use of a combination of several methods. The calculations use a model based on two methods: the magnetic wall model (sometimes called the semi-open resonator model) [31] and the finite element method (FEM), implemented in the commercial ANSYS HFSS package [32]. The following parameters were selected as significant variables: t – the gap between the dielectric substrate and the grounded base, and ε_r – the relative dielectric permittivity of the substrate itself. The substrate thickness parameter h was excluded from the variable parameters, since the thin substrate approximation is used exclusively for calculating the parameters of real antennas $h << \lambda_r$, where λ_r is the resonant wavelength of the excited oscillations. This approximation minimizes the possibility of surface waves being excited in the dielectric layer of the substrate [33].

Considering all physical aspects affecting the antenna's operating mode, the natural first step in the study would be to examine the spectral composition of the oscillations excited in the structure. It is the presence of certain types of oscillations and their mutual influence (taking into account possible dispersion) that will determine the potential capabilities of such an antenna.

The main variable parameter selected t is the distance between the dielectric substrate and the grounded base. This parameter will have a decisive influence on the entire spectral composition, since with a fixed geometry, the resonant frequencies of the microstrip patch itself and the slot discontinuities will not change, and a change in the dielectric permittivity of the substrate itself can only lead to a trivial shift in the characteristics along the frequency axis (without changing the spectral composition). Figure 2 shows the spectral characteristics of the antenna when the parameter t varies in the frequency range from 0.7 GHz to 13 GHz.

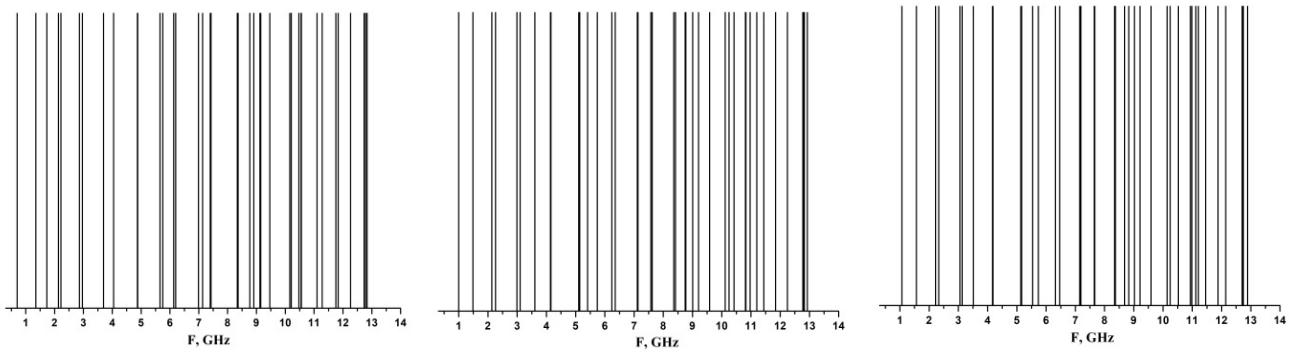

$\varepsilon_r = 2.4, t = 1\ mm$ $\varepsilon_r = 2.4, t = 1.5\ mm$ $\varepsilon_r = 2.4, t = 2\ mm$

Figure 2. Spectral characteristics of the antenna with parameter t variation

The characteristics given include 40 spectral lines in this range. The relative error in calculating the natural resonance frequencies does not exceed 10^{-7}, yielding a maximum error of no more than 1.4 kHz in the high-frequency part of the range under consideration.

A comparative analysis of the characteristics allows us to draw a general conclusion that, with the selected parameter t values, the radiating structure can operate in various modes: single-frequency with relatively narrow bands (corresponding to single spectral lines), multi-frequency with relatively wide bands (corresponding to frequency bands with a condensed spectrum or to individual frequencies with degenerate types of oscillations), and mixed mode. Modeling the spectrum above 13 GHz is not advisable due to strong spectral condensation and degenerate oscillation types, which greatly complicate type identification.

The conclusion about possible operating modes is illustrated by comparing the mutual arrangement of spectral lines in the characteristic near frequencies of 5.1 GHz and 7.5 GHz at a fixed value of the parameter t (for example, at $t = 1.5\ mm$). Near these frequencies, the spectral lines are located quite close to each other (5.10379 GHz, 5.13788 GHz and 7.5732 GHz, 7.61883 GHz), and there is no degeneration. It is precisely near these frequencies that the antenna can operate effectively. It can be argued that the value $t = 1.5\ mm$ is optimal in terms of spectral characteristics.

Another indirect indication of the optimality of certain parameter values is the structure of current densities on the surfaces of radiating apertures. The efficiency of their excitation may indicate the possibility of forming the necessary field distributions in the far field. Fig. 3 shows the structures of current density distributions on the surfaces of apertures (in the background, you can see the distribution of current densities on the surface of the grounded plane and on the slot discontinuities in it).

Frequencies close to the natural frequencies in the spectrum were selected for distribution, with a parameter value of $t = 1.5\ mm$. As can be seen from the distributions shown, the excitation of the aperture elements is sufficiently intense and sufficiently uniform. There are only slight differences in the excitation intensity of the slot log-periodic aperture element most distant from the microwave energy input point. Evidence that the ring-shaped slot discontinuities in the grounding screen actively influence on the formation of the radiated fields and other characteristics is their sufficiently effective excitation.

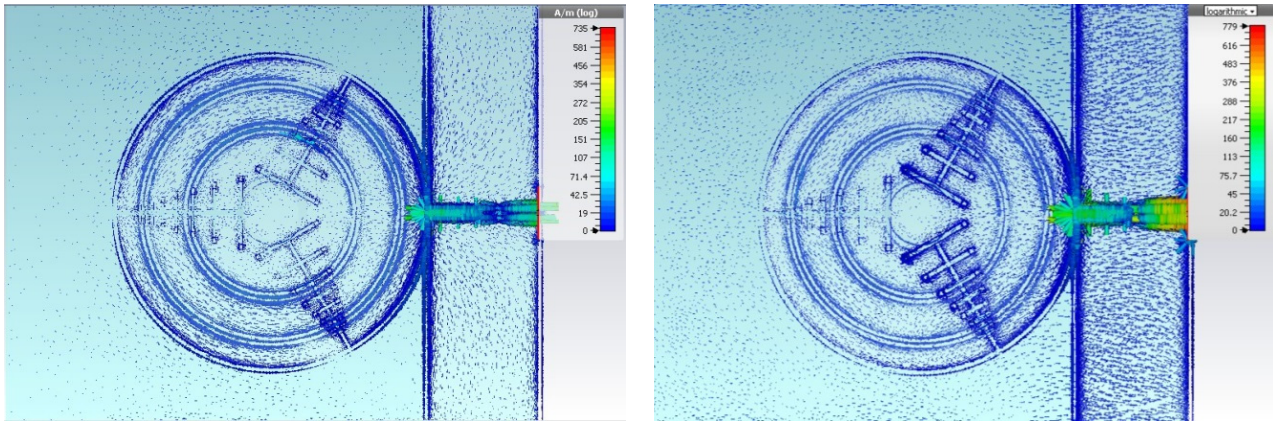

$F = 5.138$ GHz $F = 7.573$ GHz

Figure 3. Distribution of current densities on radiating apertures

The peculiarities of the current density distribution on the central conductor of the coplanar line necessitate additional research of the degree of antenna matching with external circuits. In addition, the degree of matching will indirectly indicate the efficiency of aperture excitation.

Fig. 4 shows the dependencies $|S_{11}|$ in the frequency range under consideration on the variable parameters t and ε_r. These dependencies allow us to assess the nature of the influence of the selected variable parameters on the reverse loss modulus, the presence of satisfactory matching bands, and their width.

Both dependencies are oscillatory in nature, with a significantly greater number of sharp fluctuations in value $|S_{11}|$ observed depending on ε_r. Absolute minima in dependencies $|S_{11}|$ on t at a fixed $\varepsilon_r = 2.4$ are observed near certain natural frequencies. And, if near the frequency $F = 5.5$ GHz the frequency distance of the minima is about 200 MHz, then near the frequency $F = 7.5$ GHz the distance does not exceed 80 MHz. In this situation, we can say that value of $|S_{11}|$ practically does not depend on the distance to the ground plane. The value ε_r has a significantly greater influence on the characteristic of $|S_{11}|$. If at a low value of $\varepsilon_r = 1.1$ the characteristic has a fairly wide frequency band with an acceptable level of matching (near the frequency $F = 6.5$ GHz, $\Delta F \approx 778$ MHz).

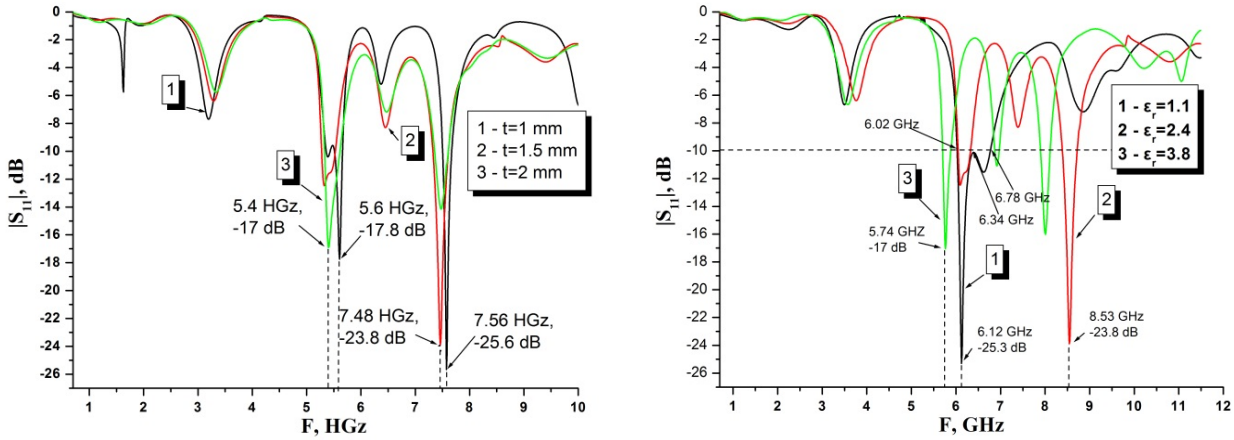

$\varepsilon_r = 2.4$ $t = 1.5\,mm$

Figure 4. Dependencies of $|S_{11}|$ on variable parameters t and ε_r

At the value of $\varepsilon_r = 2.4$ the band near this spectral line narrows significantly, but a relatively narrow band appears near the spectral line at a frequency of $F = 7.5$ GHz. That is, with this value of relative dielectric permittivity, the antenna can already operate in dual-band mode. A further increase ε_r to a value of 3.8 leads to the appearance of three narrow bands with an acceptable level of matching. However, when moving away from the center frequencies of these bands, there are quite sharp changes in the value $|S_{11}|$, which is generally unacceptable.

The functional purpose of any antenna is to form fields with specified energy characteristics in a certain part of space. These characteristics are: directivity pattern, gain coefficient, polarization characteristics. The synthesis of antennas taking these characteristics into account has always been a complex electrodynamic task, since each of the characteristics is described by a function that is multi-parametric, depending on the type of antenna, the features of the

form factor of the radiating apertures, the material constants of the substrates (in the case of planar antennas), and the possible presence of auxiliary structural elements.

Fig. 5 shows the directional patterns at a frequency of $F = 7.5$ GHz with variation of the parameter t. Curve 1 corresponds to the value $t = 1\,mm$, curve 2 corresponds to $t = 1.5\,mm$, and curve 3 corresponds to $t = 2\,mm$. The curves are normalized to the absolute maximum (observed at $t = 1.5\,mm$) to enable the evaluation of radiation efficiency.

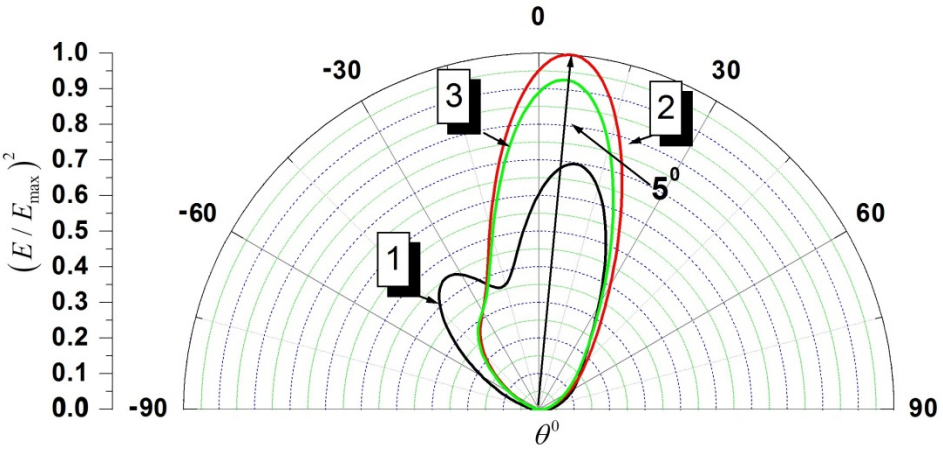

Figure 5. Directivity diagrams in the angular plane with parameter t variation

As can be seen from the figure, the distance to the grounded plane has a significant effect on both the shape of the directional pattern and the level of radiated power. At a short distance ($t = 1\,mm$), the pattern has an almost two-lobe shape (curve 1). The main lobe is shifted relative to the normal by an angle of 9^0, and the amplitude is 0.69 of the maximum value. As the distance increases (curve 2 – $t = 1.5\,mm$, curve 3 – $t = 2\,mm$), the patterns transform into single-lobe patterns, the offset from the normal is practically the same and is 5^0, and the maximum amplitude is observed at $t = 1.5\,mm$, while the width of the main lobe at a level of 0.707 is 27.8^0. Increasing the distance to the grounded plane to 2 mm leads to a slight narrowing of the main lobe.

It is clear that the total diagram is formed taking into account both elevation dependence and azimuthal dependence. Figure 6 shows two 3D directional diagrams at a frequency of $F = 7.5$ GHz for two values of the parameter t.

Analysis of the diagrams shows that, in principle, the type of diagrams is the same and largely repeats the type of diagrams in the elevation plane (Fig. 5). However, the amplitude values differ significantly, which indicates that the azimuthal components of the fields vary greatly.

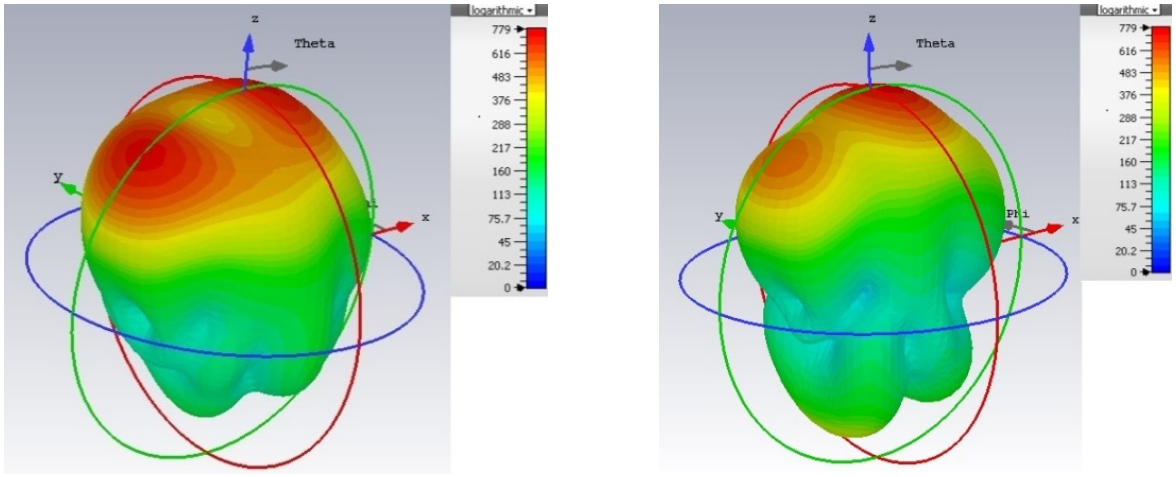

$t = 1.5\,mm$ $t = 2\,mm$

Figure 6. 3D directional diagrams at a frequency of GHz with parameter variation

Another energy parameter that determines an antenna's efficiency is the gain coefficient. Any antenna must provide an acceptable input signal level for subsequent processing. An important requirement for this characteristic is maintaining certain values above a specified level. Fig. 7 shows the dependence of the gain coefficient on the variation of the parameter t.

The behavior of the gain coefficient dependencies when varying the parameter t in the frequency range under consideration is fairly uniform. In the frequency range below 1.5 GHz, the gain coefficient values either fluctuate near zero or are negative. This behaviour is primarily due to the strong mismatch between the antenna and the exciting coplanar line (Fig. 4). With increasing frequency, a monotonic increase in the value of α begins. The maximum values for all values of the parameter α are reached near the frequency $F = 8.3$ GHz. From the point of view of the maximum gain coefficient, the optimal value is $t = 1.5\,mm$ with $\alpha = 9.22$ dBi.

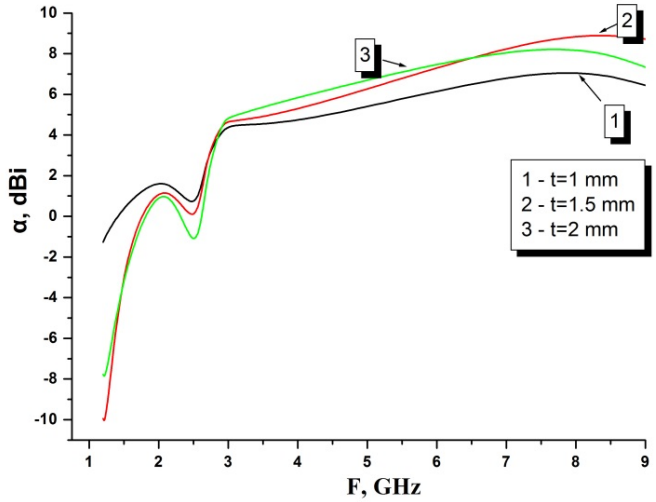

Figure 7. Dependencies of the antenna gain coefficient with parameter t variation

Another important energy characteristic is the so-called polarization characteristic, which shows the possibility of forming fields with a given polarization for transmission (reception). If we focus on the criterion of universality, then an antenna with circular (or elliptical, close to circular) polarization would be preferable. In most known designs, planar patch antennas form linearly polarized radiated fields, unless complex apertures, auxiliary elements or special excitation methods are used. Fig. 8 shows the polarization characteristics (according to the IEEE criterion in dB) for variations in the parameters t, $F = 7.5$ GHz $\varepsilon_r = 2.4$.

Figure 8 confirms the existence of a fairly strong dependence of the ellipticity coefficient function η on the observation angle θ (the angle of elevation, measured from the normal to the antenna plane). The optimal option in terms of minimum ellipticity coefficient is the close location of the grounding plane ($t = 1\,mm$). At an observation angle $\theta = 68.3^0$, an ellipticity coefficient of $\eta = 1.2$ dB is achieved. Moreover, in the angle range from 55^0 to 78.5^0, the ellipticity coefficient does not exceed 3 dB.

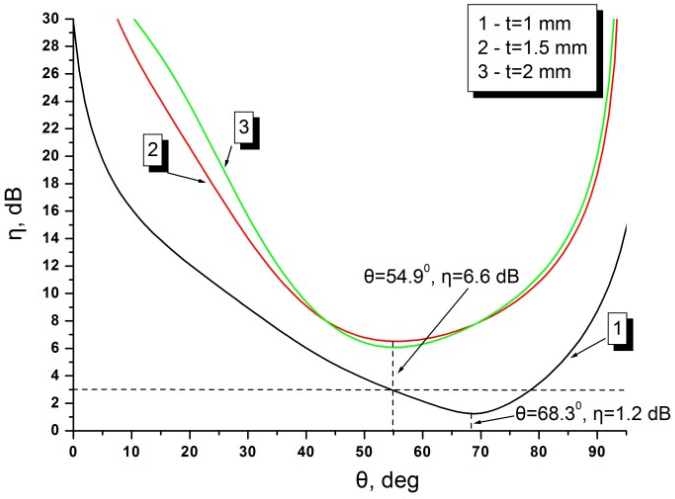

Figure 8. Polarization characteristics with parameter t variation

When the observation angle deviates from these values, the polarization becomes linear. For other tested parameter values, the ellipticity coefficients do not differ significantly from each other. The minimum achievable value is $\eta = 6.6$ dB at an observation angle of $\theta = 54.9^0$, which is quite far from the desired ellipticity coefficient value.

CONCLUSIONS

This paper presents the results of numerical modelling of the main characteristics of a patch antenna with a complex radiating aperture in the form of three sets of slot discontinuities in a microstrip disc with a log-periodic profile and oriented at an angle of 120^0 relative to each other. A ground plane located at a certain distance from a dielectric substrate with three ring slot discontinuities is used as an auxiliary element to influence the main characteristics. Using procedures for optimizing the electrodynamic characteristics of the antenna according to selected variable parameters, it was established that it is necessary to use a certain compromise set of parameters capable of ensuring the formation of the specified distributions of radiated (received) fields, an acceptable level of matching with external circuits, and acceptable values of the gain coefficient.

Acknowledgements

This work was supported by the Ministry of Education and Science of Ukraine, grant 0126U000999.

ORCID

Sergey A. Pogarsky, https://orcid.org/0000-0003-0833-1421; **Dmitry V. Mayboroda,** https://orcid.org/0000-0002-9564-2369
Mikhail V. Nesterenko, https://orcid.org/0000-0002-1297-9119

REFERENCES

[1] K.-L. Wong, *Compact and Broadband Microstrip Antennas*, (John Wiley & Sons, 2002). https://doi.org/10.1002/0471221112
[2] G. Kumar, and K.P. Ray, *Broadband microstrip antennas*, (Artech House, 2003). http://read.pudn.com/downloads150/ebook/652719/Broadband%20microstrip%20antennas.pdf
[3] R. Garg, P. Bhartia, I. Bahl, and A. Ittipiboon, *Microstrip Antenna Design Handbook*, (Artech House, 2001). https://uodiyala.edu.iq/uploads/PDF%20ELIBRARY%20UODIYALA/EL37/Microstrip%20Antenna%20Design%20Handbook.pdf
[4] J. Liu, Q. Xue, H. Wong, H.W. Lai, and Y. Long, IEEE Trans. Antennas Propag., **61**, 11 (2013). https://doi.org/10.1109/TAP.2012.2214996
[5] X. Ma, Y Zong, P. Zhang, J. Chen, and Z. Ren, IEEE Trans. Antennas Propag. **74**, 38 (2026). https://doi.org/10.1109/TAP.2025.3623329
[6] S. Lin, Progress in Electr. Res. **90**, 369 (2009). http://dx.doi.org/10.2528/PIER09020503
[7] R. Li, Y.-X. Guo, B. Zhang, and G. Du, IEEE Antennas and Wireless Propag. Lett. **16**, 2566 (2017). https://doi.org/10.1109/LAWP.2017.2734246
[8] D.V. Maiboroda, and S.A. Pogarsky, Telecom. and Radio Eng. **73**(19), 1713 (2014). https://doi.org/10.1615/TelecomRadEng.v73.i19.20
[9] S.A. Pogarsky, D.V. Mayboroda, and S.M. Mikhaliuk, East Eur. J. Phys. (4), 274 (2023). https://doi.org/10.26565/2312-4334-2023-4-34
[10] T.-S. Wang, C.-Z. Du, H.-F. Shu, and Z.-H. Yue, PIER C, **140**, 127 (2024). https://doi.org/10.2528/PIERC23111602
[11] Y. Liu, S. Gong, and H.-B. Zhang, in: *2006 IEEE Antennas and Propagation Society International Symposium (IEEE, 2006)*, 2603–2606. https://doi.org/10.1109/APS.2006.1711133
[12] S. A. Pogarsky, D. V. Mayboroda, and S. N. Mykhaliuk, in: *2024 IEEE 29th International Seminar/Workshop on Direct and Inverse Problems of Electromagnetic and Acoustic Wave Theory (DIPED)*, (IEEE, 2024), pp. 103–106. https://doi.org/10.1109/DIPED63529.2024.10706159
[13] S. Zhang, and D. Zhao, *Aerospace materials handbook*, (CRC Press, 2012). https://www.zlibrary.to/filedownload/aerospace-materials-handbook-2.
[14] R.P. Owens, J.E. Aitken, and T.C. Edwards, IEEE Trans. MTT, **24**, 499 (1976). https://doi.org/10.1109/TMTT.1976.1128887
[15] Y. Tokumitsu, M. Ishizaki, M. Iwakuni, and T. Saito, IEEE MTT, **31**, 121 (1983). https://doi.org/10.1109/TMTT.1983.1131445
[16] P. Muthusamy, S. Shaik, and M. Reddy, in: *2025 IEEE Wireless Antenna and Microwave Symposium (WAMS)*, (2025). https://doi.org/10.1109/WAMS64402.2025.11158849
[17] S. Yuanhua, and L. Yihe, in: *2019 2nd International Conference on Communication Engineering and Technology (ICCET)*, (2019). https://doi.org/10.1109/ICCET.2019.8726870
[18] B. Mohamadzade, Roy B. V. B. Simorangkir, R. Maqsood Hashmi, Y. Chao-Oger, M. Zhadobov, and Ronan Sauleau, IEEE Antennas and Wireless Propag. Lett. **19**, 203 (2020). https://doi.org/10.1109/LAWP.2019.2958036
[19] N. Khalid, S. Z. Ibrahim, and M. N. A. Karim, in: *2016 3rd International Conference on Electronic Design (ICED)*, (2016). https://doi.org/10.1109/ICED.2016.7804637
[20] O. A. Al Kaladi, and A. S. M. Alqadami, in: *2025 IEEE International RF and Microwave Conference (RFM)*, (2025). https://doi.org/10.1109/RFM67034.2025.11284496
[21] X. Zhang, Y. Liu, J. Q. Zhu, and W. Cui, in: *2023 16th UK-Europe-China Workshop on Millimetre Waves and Terahertz Technologies (UCMMT)*, (2023). https://doi.org/10.1109/UCMMT58116.2023.10418967
[22] W.-S. Yoon, D.-H. Lee, K.-J. Lee, S.-H. Kim, S.-M. Han, and Y.-S. Kim, in: *2009 Loughborough Antennas & Propagation Conference*, (2009). https://doi.org/10.1109/LAPC.2009.5352514
[23] H. J. Kim, S. M. Kim, J. M. Son, and W. G. Yang, in: *2005 Asia-Pacific Microwave Conference Proceedings*, (2005). https://doi.org/10.1109/APMC.2005.1606902
[24] T.-C. Yo, C.-M. Lee, and C.-H. Luo, in: *2007 International workshop on Antenna Technology: Small and Smart Antennas Metamaterials and Applications*, (2007). https://doi.org/10.1109/IWAT.2007.370167
[25] G. Idayachandran, E. Ramassamy, M. Sivaraj, and V. Rajesh, in: *2019 IEEE International Conference on System, Computation, Automation and Networking (ICSCAN)*, (2019). https://doi.org/10.1109/ICSCAN.2019.8878715
[26] J. P. Zhang, and J. J. Mao, in: *2020 International Conference on Microwave and Millimeter Wave Technology (ICMMT)*, (2020). https://doi.org/10.1109/ICMMT49418.2020.9386991

[27] R. George, C. R. S. Kumar, and S.A. Gangal, in: *2016 International Conference on Communication and Signal Processing (ICCSP)*, (2016). https://doi.org/10.1109/ICCSP.2016.7754451
[28] N. EL Anzoul, Y. K. Bekali, and K. Minaoui, in: *2025 12th International Conference on Wireless Networks and Mobile Communications (WINCOM)*. (2025). https://doi.org/10.1109/WINCOM65874.2025.11313447
[29] M. Schubler, M. Maasch, C. Damm, and R. Jakoby, in: *2009 European Microwave Conference (EuMC)*, (2009). https://doi.org/10.23919/EUMC.2009.5296144
[30] S. Sharma, M. Kumar, H. Nigam, and M. Mathur, in: *2021 IEEE Indian Conference on Antennas and Propagation (InCAP)*, (2021). https://doi.org/10.1109/InCAP52216.2021.9726406
[31] G. Kompa, and R. Mehran, Electron. Lett. **11**, 459 (1975). https://doi.org/10.1049/el:19750352
[32] Ansoft HFSS /ANSYS Academic Research HF (5 tasks): 1 task(s) Permanent Customer #1076710.
[33] V.R. Komanduri, V.R. Jackson, J.T. Williams, and A.R. Mehrotra, IEEE Trans. on Antennas and Propag. **61**, 2887 (2014). https://doi.org/10.1109/TAP.2013.2254441

ХАРАКТЕРИСТИКИ ВИПРОМІНЮВАНИХ ПОЛІВ, СФОРМОВАНИХ ПАТЧ-АНТЕНОЙ ЗІ СКЛАДНОЮ АПЕРТУРОЮ

Сергій О. Погарський, Дмитро В. Майборода, Михайло В. Нестеренко, Сергій М. Михалюк, Олександр А. Білошенко
Харківський національний університет імені В.Н. Каразіна, майдан Свободи, 4, Харків, Україна, 61022

У статті розглянуто питання, пов'язані з моделюванням електродинамічних характеристик смужкової антени на основі мікросмужкового дискового резонатора зі складною топологією випромінюючої апертури у вигляді трьох щілинних логарифмічно-періодичних неоднорідностей, орієнтованих під кутом 120^0 з масштабним коефіцієнтом $\tau = 0,8$ і коефіцієнтом кроку $\sigma = 0,15$. У заземленій основі на певній відстані від діелектричної підкладки розташовані три концентричні кільцеві щілинні розриви, центри яких збігаються з центром мікросмужкового диска. Антена живилася відрізком компланарної лінії зі ступінчастим профілем центрального провідника. У розрахунках використовувалася модель, побудована на основі двох методів: моделі магнітної стінки (модель напіввідкритого резонатора) та методу скінченних елементів. Після проведення оптимізаційних процедур для вибраних параметрів було встановлено, що для отримання необхідних характеристик необхідні компромісні набори параметрів.

Ключові слова: *кільцевий резонатор; щілинний розрив; компланарна лінія; узгодження; частотні характеристики; енергетичні характеристики*